PHYSICS AND CHEMISTRY OF SOLID STATE
V. 23, No. 2 (2022) pp. 353-360
Section: Physics

DOI: 10.15330/pcss.23.2.353-360

Vasyl Stefanyk Precarpathian National University

ФІЗИКАІХІМІЯТВЕРДОГОТІЛА
Т. 23, № 2 (2022) С. 353-360
Фізико-математичні науки

PACS:78.20.Ci; 72.80.Ng ISSN 1729-4428

Alaa J. Kadham Algidsawi[1], Ahmed Hashim[2], Aseel Hadi[3], Majeed Ali Habeeb[2], Hussein Hakim Abed[4]

Influence of MnO_2 Nanoparticles Addition on Structural, Optical and Dielectric Characteristics of PVA/PVP for Pressure Sensors

[1]*Department of Soil and Water, College of Agriculture, AL-Qasim Green University, Babylon, Iraq*
[2]*Department of Physics, College of Education for Pure Sciences, University of Babylon, Babylon, Iraq, ahmed_taay@yahoo.com*
[3]*University of Babylon, College of Materials Engineering, Department of Ceramic and Building Materials, Iraq*
[4]*Department of Physics, College of Science, University of Babylon, Babylon, Iraq*

Films of PVA/PVP/MnO_2 nanostructures were fabricated for pressure sensors fields with lightweight, flexible and low cost compare with other sensors. The structure, dielectric and optical characteristics of PVA/PVP/MnO_2 nanostructures have been studied. The results showed that the dielectric constant, dielectric loss and A.C electrical conductivity of PVA/PVP blend are enhanced with the increase in MnO_2 NPs content. The dielectric constant and dielectric loss decrease while the A.C electrical conductivity increases with the increase in frequency. The optical characteristics of PVA/PVP/MnO_2 nanostructures showed that the absorbance was rise with increasing of the MnO_2 NPs content. The indirect energy gap of PVA/PVP blend was reduced with increase in MnO_2 NPs content. The optical constants of blend are changed with the increase in MnO_2 NPs content. The pressure sensor application results of PVA/PVP/MnO_2 nanostructures showed that the electrical capacitance (C_p) increases with the rise in applied pressure.

Keywords: MnO_2, pressure sensors, energy gap, dielectric constant, conductivity.

Received 24 July2021; Accepted 4 March 2022.

Introduction

The new polymer nanocomposites production has been commonly studied by the modern fields on nanoscale inorganic additive in the food packaging approaches, barrier fields, coatings, antimicrobial, sensors, antiballistic products, conductive, and other materials. The novel generation of these nanocomposites includes carbides (B_4C, SiC, WC), nitrides (BN CrN, TiN, ZrN), borides (CrB_2, ZrB_2,WB, TiB_2), metal oxides (Y_2O_3, MgO, Al_2O_3, ZrO_2, CeO_2, Fe_2O_3, SiO_2, TiO_2), cellulose nanofibrils, carbon nanotubes, and other nanoparticles types as scatter phase. The properties and characteristics of the new nanomaterials are affected by the kind of additive employed by the polymer matrix. The applications include many fields like electronics, aerospace, military, vehicles, marine and medicine [1]. The transition metals oxides are an significant group of semiconductors have functions in solar energy transformation, magnetic storage media, catalysis and electronics [2]. MnO_2 is promising green matter has involved large interests in good quality of its excellent environmental compatibility, low cost, and broad structural diversity combined with especial chemical and physical characteristics. The important fields of MnO_2 nano-scale contain alkaline batteries, gas sensors, photocatalyst, electrochemical capacitors, and smart windows [3].Polyvinyl alcohol is an important polymer, relate to its chemical and physical features. This polymer may be a film, powder, and fiber forms. PVA has a semi-crystalline nature due from the hydrogen bonds and the OH group role. Relate to its low protein adsorption properties, excellent water solubility and biocompatibility, PVA is usually employed in medical devices. Polyvinyl-pyrrolidone has a excellent stable environment, moderate electric conductivity and easy processing. PVP has a broad applications range like electrochemical devices. PVA/PVP interactions have unique characteristics which

combine the characteristics of both polymers [4]. The present work aims to prepare the PVA/PVP/MnO_2 nanostructures films to use as lightweight and low-cost pressure sensors.

I. Materials and Methods

Nanocomposites films of polyvinyl alcohol (PVA)-polyvinyl pyrrolidone (PVP)- manganese oxide (MnO_2) was fabricated by using casting method. The solution of PVA/PVP blend was prepared by the 0.5 gm of PVA and PVP with ratio 77 wt.% PVA: 23 wt.% PVP were dissolved in distilled water (20 ml) of. The MnO_2 NPs added to the blend with ratios are 1.5 %, 3 % and 4.5 %. The optical characteristics measured in range of wavelength (220 - 820) nm by spectrophotometer (UV/1800/ Shimadzu). The dielectric characteristics of films measured in frequency range (100 Hz - 5 $\times 10^6$ Hz) by LCR meter type (HIOKI 3532-50 LCR HI TESTER). The pressure sensor testing investigated by measuring the capacitance between two electrodes on the top and bottom of the sample for various pressures range (80 - 200) bar. The absorption coefficient (α) is given by [5,6]:

$$\alpha = 2.303\ (A/t), \tag{1}$$

where A: absorbance and t: sample thickness.

The energy band gap can be determined by [7]:

$$Ah\upsilon = B(h\upsilon - E_g)^r \tag{2}$$

where B: constant, hυ: photon energy, E_g: energy band gap, r = 3 for forbidden indirect transition and r = 2 for allowed indirect transition.

The refractive index (n) is given by [8]:

$$n = \frac{1+\sqrt{R}}{1-\sqrt{R}}, \tag{3}$$

where R is the reflectance.

The extinction coefficient (k) is defined by [9]:

$$k = \frac{\alpha\lambda}{4\pi}, \tag{4}$$

where λ is the wavelength of incident photon.

The dielectric constant parts: real (ε_1), and imaginary (ε_2) are calculated by the equations [10]:

$$\varepsilon_1 = n^2 - k^2 \tag{5}$$

$$\varepsilon_2 = 2nk \tag{6}$$

The optical conductivity (σ_{op}) can be calculated by the equation [11].

$$\sigma_{op} = \frac{\alpha n c}{4\pi} \tag{7}$$

The dielectric constant (έ) is given by the equation [12]:

$$\varepsilon^- = \frac{c_p}{c_0}, \tag{8}$$

where, C_p is parallel capacitance and C_o is vacuum capacitor

The dielectric loss (ε″) can be calculated by using [13]:

$$\varepsilon'' = \acute{\varepsilon}\, D, \tag{9}$$

where D is dispersion factor.

The AC electrical conductivity can be determined by using [14]:

$$\sigma_{A.C} = w\, \varepsilon''\varepsilon_o, \tag{10}$$

where w – angular frequency.

II. Results and Discussion

Figure 1 shows the FTIR measurements of PVA/PVP/MnO_2 nanostructures. As shown in Figure 1, there is no interactions between the blend and the MnO_2 NPs. It shows broad bands at around 3257 cm^{-1} are observed related to OH groups in the blend chain. The peaks at around 1647 cm^{-1} due to the presence of such free C=O groups. The bands at around 1289 cm^{-1} due to the other bonds (C-O-C) [15].

The behavior of absorbance of pure polymeric blend and PVA/PVP/MnO_2 nanostructures with wavelength is shown in Figure 2. The absorbance of blend is rise with the increase in MnO_2 NPs content; this is relate to rise of the charges carries numbers [16,17].

The absorption coefficient is useful to show the electron transition nature. The PVA/PVP/MnO_2 nanostructures has values of absorption coefficient less than (10^4 cm^{-1}) as shown in Figure 2. The absorption coefficient of PVA/PVP/MnO_2 nanostructures is rise with the rise of MnO_2 NPs content which related to rise the charges carries numbers [18], as shown in Figure 3. Figure 3 indicates that the nanoparticles shape a continuous arrangement within the polymeric blend at high ratios [19,20]. The absorption coefficient values indicate to the PVA/PVP/MnO_2 nanostructures have indirect energy gap. Figures 4 and 5 represent the energy gap for allowed indirect and forbidden indirect transitions respectively. As shown in Figures, the energy gap are reduced with the rise in MnO_2 NPs ratio which is due to the some defects formation in the samples. These defects create the localized positions in the optical band gap and overlap. These overlaps offer evidence for reducing energy band gap when the MnO_2 NPs ratio rise in the polymeric blend [21].

The variation of extinction coefficient and refractive index with wavelength of films are shown in Figures 6 and 7 respectively. The figures indicate that the extinction coefficient and refractive index of blend are rise with the rise in MnO_2 NPs ratio. The rise of extinction coefficient and refractive index of blend related to rise the absorption coefficient and the samples density [22-25].

Figures 8 and 9 indicate to the real and imaginary of dielectric constant behavior with wavelength respectively. The real part mostly depends on n^2 because

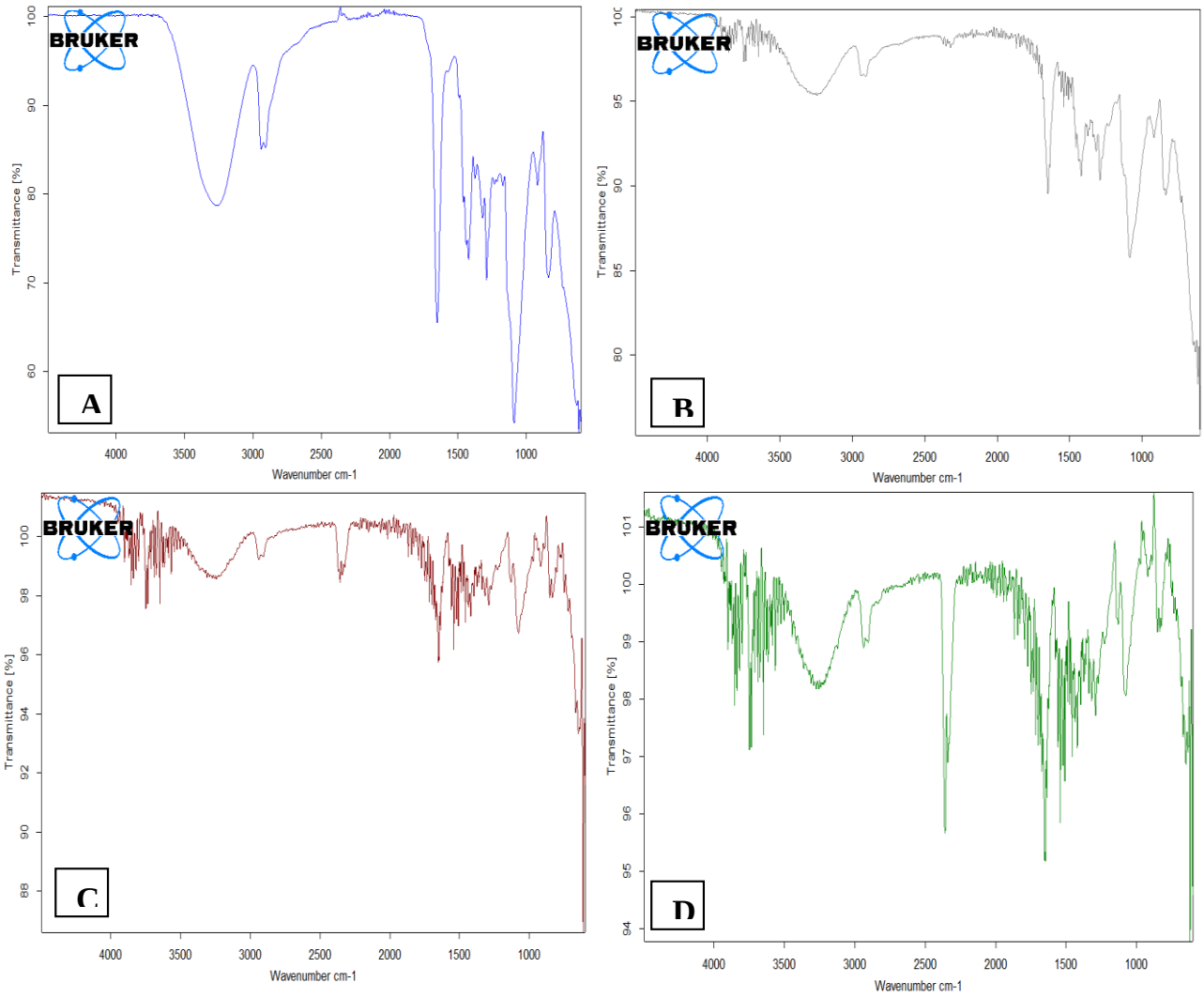

Fig. 1. FTIR spectra of PVA/PVP/MnO_2 nanostructures: A – pure blend, B – 1.5 wt.% MnO_2NPs, C – 3 wt MnO_2NPs, D – 4.5 wt.%. MnO_2 NPs.

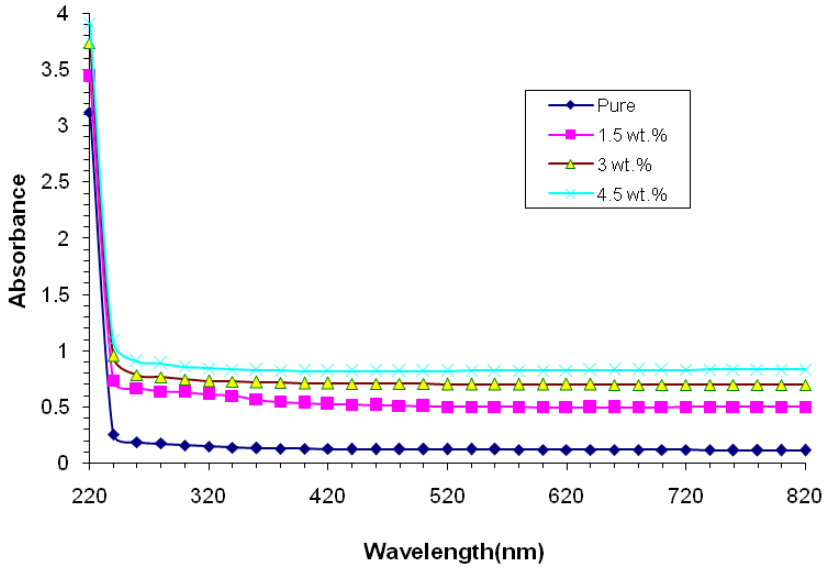

Fig. 2. Absorbance behavior of PVA/PVP/MnO_2 nanostructures with wavelength.

the k^2 values are small as compared to the n^2 values while imaginary part generally depends on the k values [26].

Figure 10 represents the optical conductivity variation of PVA/PVP/MnO_2 nanostructures with wavelength. The optical conductivity of blend rises with the increase in MnO_2 NPs ratio and photon energy. The rise in optical conductivity as MnO_2 NPs ratio increase due to reduce the energy gap [27-28].

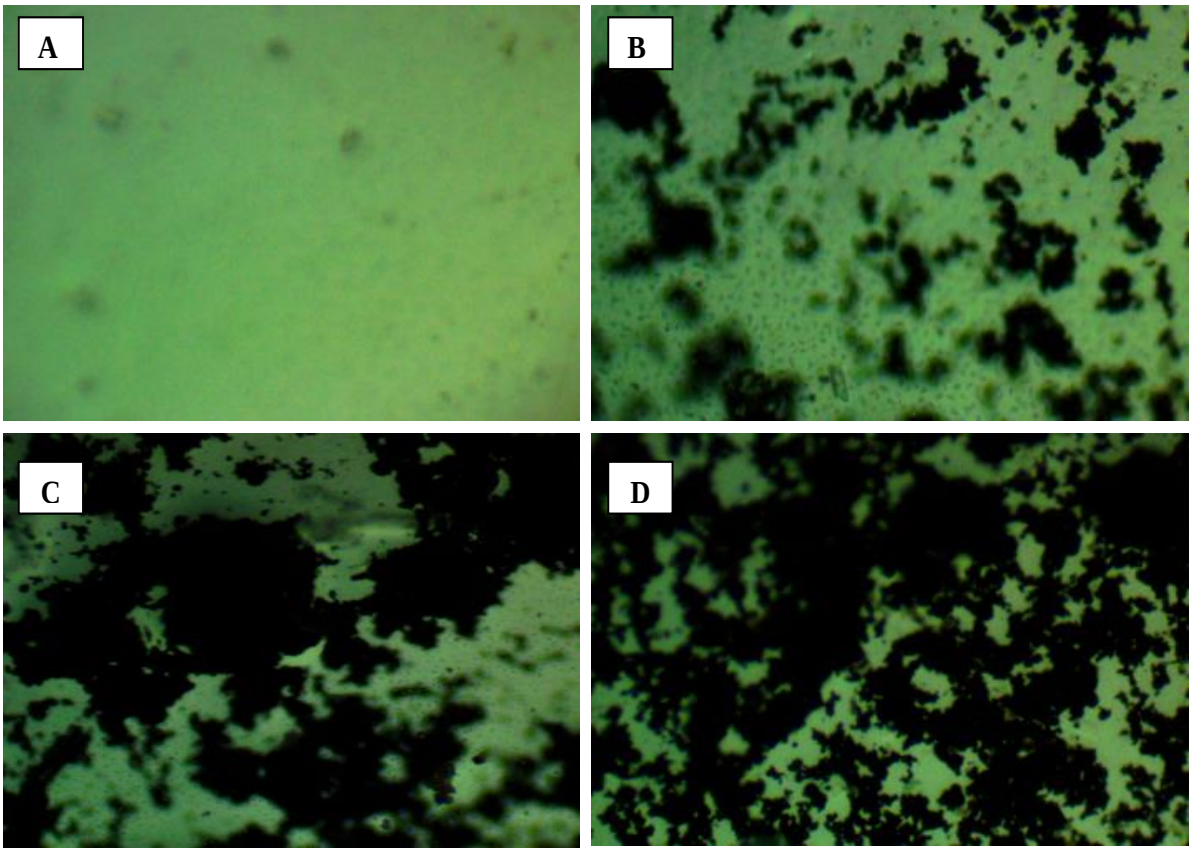

Fig. 3. Photomicrographs (x10) of PVA/PVP/MnO_2 nanostructures: A – pure blend, B– 1.5 wt.% MnO_2NPs, C – 3 wt. MnO_2NPs, D – 4.5 wt.%. MnO_2NPs.

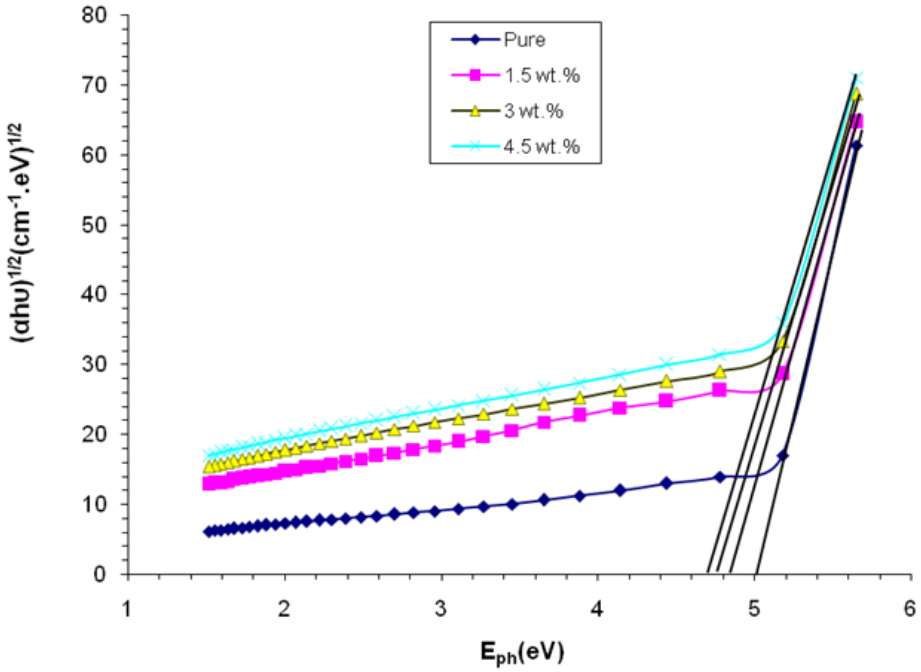

Fig. 4. Energy gap of allowed transition.

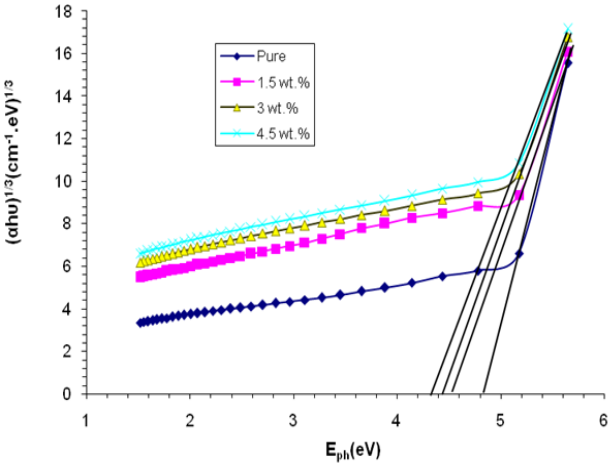

Fig.5. Energy gap of forbidden transition.

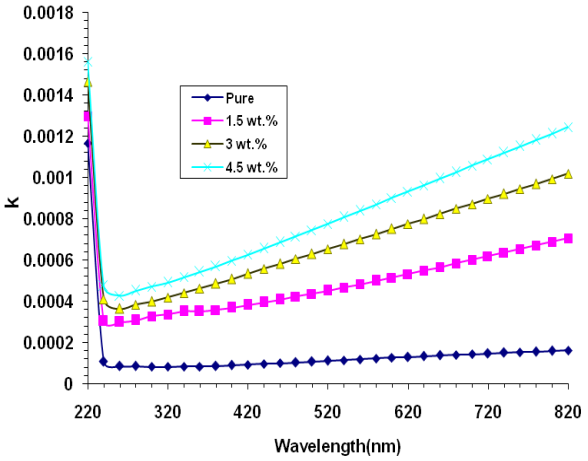

Fig. 6. Extinction coefficient variation with wavelength.

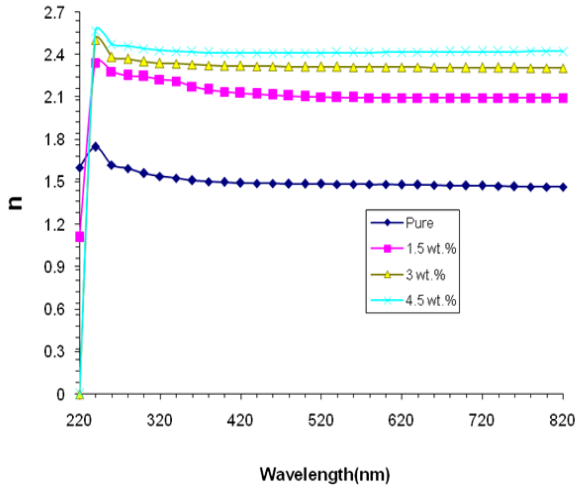

Fig. 7. Refractive index variation with wavelength.

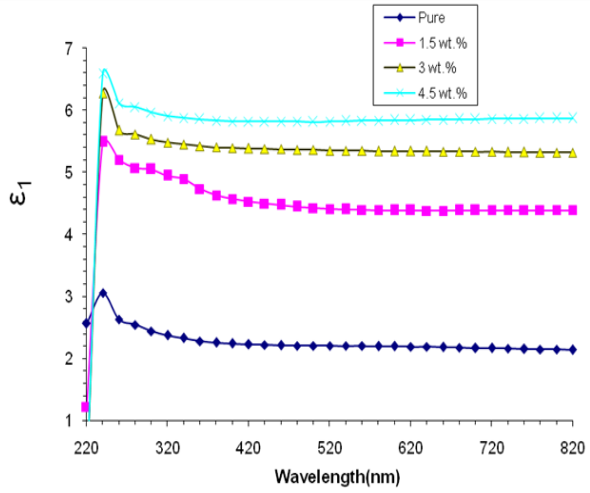

Fig. 8. Real dielectric constant behavior with wavelength.

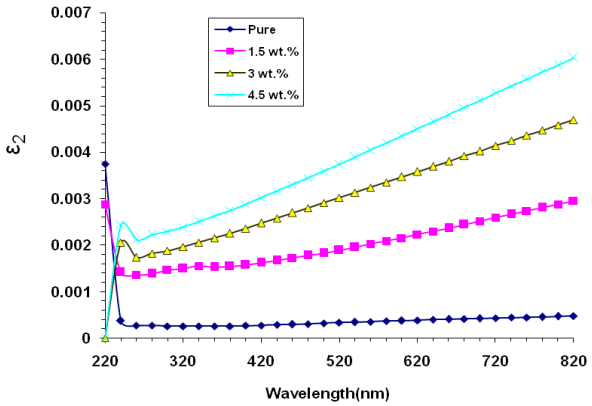

Fig. 9. Imaginary dielectric constant behavior with wavelength.

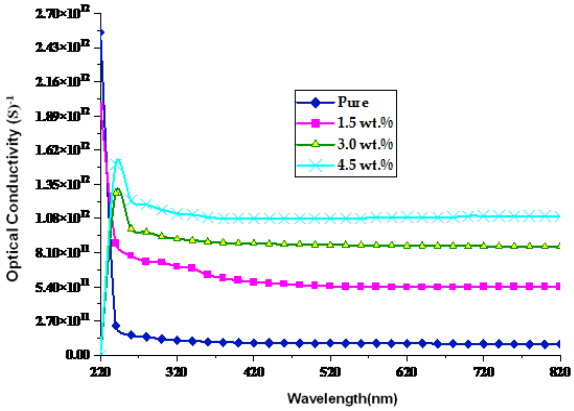

Fig. 10. Optical conductivity behavior of films with wavelength.

Figures 11-13 show the variation of dielectric constant, dielectric loss and A.C electrical conductivity of PVA/PVP/MnO_2 nanostructures with frequency respectively. From the Figures, the dielectric constant, dielectric loss and electrical conductivity of blend rise with rise in MnO_2 NPs ratio which is relate to rise of the charge carrier density in blend [29, 30]. The dielectric constant and dielectric loss reduce while the conductivity rises with the rise in frequency; this is due to the polarization effects [31]. The variation of capacitance for PVA/PVP/MnO_2 nanostructures films with pressure is shown in Figure 4. The figure indicates that the

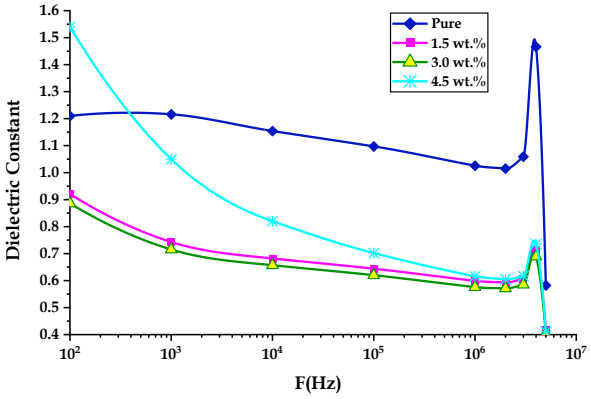

Fig.11. Dielectric constant behavior of PVA/PVP/MnO_2 nanostructures with frequency.

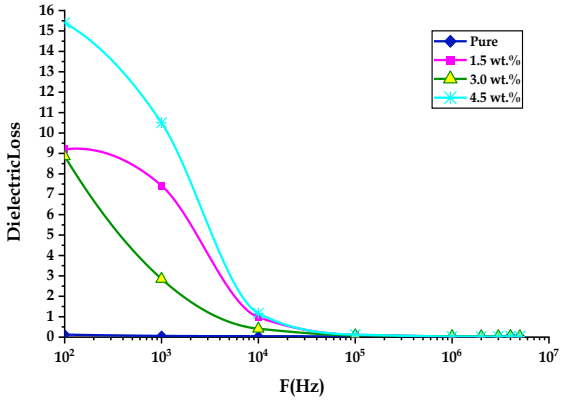

Fig. 12. Dielectric loss variation of PVA/PVP/MnO_2 nanostructures with frequency.

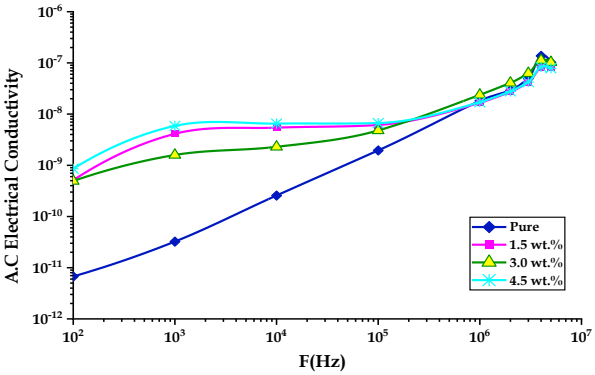

Fig. 13. Electrical conductivity variation of PVA/PVP/MnO_2 nanostructures with frequency.

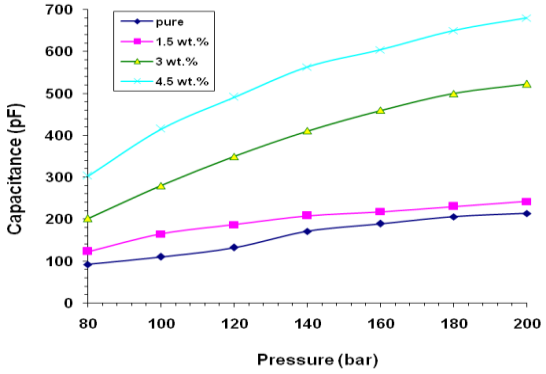

Fig. 14. Capacitance variation of PVA/PVP/MnO_2 nanostructures with pressure.

capacitance rises with the rise in pressure. When the pressure is applied to film, it led to mechanical deformation and charges displacement. An electric field will produce and consequently voltage may be detected on the lower and upper film surface. When stress is removed, the voltage will disappear. This fact is called direct piezoelectric effect. Conversely, the internal production of mechanical strain of the film resulting from an applied electrical field is called reverse piezoelectric effect [32].

Conclusions

The results of optical characteristics showed that the optical absorbance of PVA/PVP blend rises with the rise in the MnO_2 NPs ratio. The energy gap of blend reduces with the rise in MnO_2 NPs content. The optical constants (absorption coefficient, extinction coefficient, refractive index, dielectric constants parts and optical conductivity) of PVA/PVP blend are rise with increasing of the MnO_2 NPs content. The dielectric constant, dielectric loss and A.C electrical conductivity of PVA/PVP blend rise with the rise in MnO_2 NPs content. The dielectric constant and dielectric loss of PVA/PVP/MnO_2 nanostructures reduce while the conductivity rises with the rise in frequency. The results of PVA/PVP/MnO_2 nanostructures application for pressure sensors indicated that the nanostructures films have highly sensitive for pressure.

Alaa J. Kadham Algidsawi –Professor, Department of Soil and Water, College of Agriculture, AL-Qasim Green University;
Ahmed Hashim –Professor, Department of Physics, University of Babylon;
Aseel Hadi – Assistant Professor, Department of Ceramic and Building Materials, College of Materials Engineering, University of Babylon;
Majeed Ali Habeeb – Professor, Department of Physics, University of Babylon;
Hussein Hakim Abed – Assistant Professor, Department of Physics, College of Science, University of Babylon.

[1] F.J. Tommasini, L.d.C. Ferreira, L.G.P. Tienne, V.d.O. Aguiar, M.H.P.d. Silva, L.F.d.M. Rocha, M.d.F.V. Marques, Materials Research 21, 6 (2018); https://doi.org/10.1590/1980-5373-MR-2018-0086.
[2] S.G. Rejith and C. Krishnan, Advances in Applied Science Research 4, 2 (2013); www.pelagiaresearchlibrary.com.

[3] S. Akbari, M.M. Foroughi and M. Ranjbar, J. ofNanomedicine& Nanotechnology 9, 3 (2018); https://doi.org/10.4172/2157-7439.1000498.
[4] H.M. Zidan, E.M. Abdelrazek, A.M. Abdelghany, A.E. Tarabiah, J. of Materials Research and Technology 8, 1 (2019); https://doi.org/10.1016/j.jmrt.2018.04.023.
[5] M. O. Farea, A. M. Abdelghany and A. H. Oraby, RSC Adv. 10 (2020), https://doi.org/10.1039/d0ra07601e.
[6] S. Hadi, A. Hashim and A. Jewad, Australian Journal of Basic and Applied Sciences 5(9), 2192 (2011).
[7] A M A HenaishAndA S Abouhaswa, Bull. Mater. Sci. 43 (2020), https://doi.org/10.1007/s12034-020-2109-5.
[8] S. Agarwal, Y. K. Saraswat and V. K. Saraswat, Open Physics Journal 3, 63-72 (2016),https://doi.org/10.2174/1874843001603010063.
[9] N. Mahfoudh, K. Karoui and A. Ben Rhaiem,RSC Adv. 11 (2021), https://doi.org/10.1039/d1ra03652a.
[10] P. O. Amin, K. A. Ketuly, S. R. Saeed, F. F. M. sharif, M. D. Symes, A. Paul and K. Sulaiman, BMC Chemistry 15 (2021), https://doi.org/10.1186/s13065-021-00751-4.
[11] G. Veena, B. Lobo, Turkish Journal of Physics 43, 337-354 (2019).
[12] H. Shivashankar, K. A. Mathias, P. R. Sondar, M. H. Shrishail, and S. M. Kulkarni, J Mater Sci: Mater Electron32, 28674–28686 (2021).
[13] A. A. Abdelmalik, A. Sadiq, & U. Sadiq, J. Phys. Sci. 31(1), 1–14 (2020), https://doi.org/10.21315/jps2020.31.1.1.
[14] S. Ishaq, F. Kanwal, S. Atiq, M. Moussa, U. Azhar and D. Losic, Materials 13, (2020), https://doi.org/10.3390/ma13010205.
[15] A. Hashim, I.R. Agool and K.J. Kadhim, J. of Materials Science: Materials in Electronics 29, 12 (2018); https://doi.org/10.1007/s10854-018-9095-z.
[16] A. F Al-Shawabkeh, Z. M Elimat and K. N Abushgair, Journal of Thermoplastic Composite Materials (2021), https://doi.org/10.1177/08927057211038631.
[17] A. Hashim,K.H.H. Al-Attiyah,S.F. Obaid, Ukr. J. Phys. 64, 2 (2019); https://doi.org/10.15407/ujpe64.2.157.
[18] S. Salman, N. Bakr and M. H. Mahmood, International Journal of Current Research 6(11), 9638-9643, (2014).
[19] H. Abduljalil, A. Hashim, A. Jewad, European Journal of Scientific Research 63, 2 (2011).
[20] K.H.H. Al-Attiyah, A. Hashim, S.F. Obaid, International Journal of Plastics Technology 23, 1 (2019); https://doi.org/10.1007/s12588-019-09228-5.
[21] A. Hashim and M.A. Habeeb, Transactions on Electrical and Electronic Materials 20, (2019); https://doi.org/10.1007/s42341-018-0081-1.
[22] J.J. Mathen, G.P. Joseph, J. Madhavan, International Journal of Engineering Development and Research 4, 3 (2016); www.ijedr.org.
[23] S. Agarwal, Y.K. Saraswat and V.K. Saraswat, Open Physics J., 3, 63 (2016); https://doi.org/10.2174/1874843001603010063.
[24] A. Hashim, Journal of Inorganic and Organometallic Polymers and Materials 30, (2020); https://doi.org/10.1007/s10904-020-01528-3.
[25] F.A. Jasim, A. Hashim, A.G. Hadi, F. Lafta, S.R. Salman and H. Ahmed, Research Journal of Applied Sciences 8-9, 439 (2013).
[26] H. M. Zidan, E. M. Abdelrazek, A. M. Abdelghany, A. E. Tarabiah, j. mater. Res. Technol. 8(1), 904–913 (2019).
[27] A. Hashim, Z.S. Hamad, Egypt. J. Chem. 63, 2 (2020);https://doi.org/10.21608/EJCHEM.2019.7264.1593.
[28] C. Tyagi and A. Devi, J. of Advanced Dielectrics 8(3) (2018), https://doi.org/10.1142/S2010135X18500200.
[29] S. Latha Pala, S. N. Varma, N. K. Jyothi and K. V. Kumar, J. Indian Chem. Soc. 96, 182-184, (2019).
[30] A. Hashim, H.M. Abduljalil, H. Ahmed, Egypt. J. Chem., 63, 1 (2020); https://doi.org/10.21608/EJCHEM.2019.10712.1695.
[31] A. Hashim, J Mater Sci: Mater Electron 32, (2021); https://doi.org/10.1007/s10854-020-05032-9.
[32] A. Hashimand A. Hadi, Sensor Letters 15, (2017); https://doi.org/10.1166/sl.2017.3910.

А.Й. Кадхам Алжідсаві[1], А. Хашім[2], А. Хаді[3], М.А. Хабіб[2], Х.Х. Абед[4]

Вплив введення наночастинок MnO_2 на структурні, оптичні та діелектричні характеристики PVA/PVP для датчиків тиску

[1]*Кафедра ґрунту та води, сільськогосподарський коледж, Університет Гріна Аль-Касіма, Вавилон, Ірак*
[2]*Кафедра фізики, університет Вавилону, Вавилон, Ірак, ahmed_taay@yahoo.com*
[3]*Коледж інженерії матеріалів, кафедра кераміки та будівельних матеріалів, університет Вавилону, Вавилон, Ірак*
[4]*Фізичний факультет, Науковий коледж університету Вавилону, Вавилон, Ірак*

Наноструктуровані плівки PVA/PVP/MnO_2 виготовлено для застосування у якості датчиків тиску, як гнучкі та недорогі, порівняно із іншими датчиками. Досліджено структуру, діелектричні та оптичні характеристики наноструктур PVA/PVP/MnO_2. Дослідження показали, що діелектрична проникність, діелектричні втрати та електрична провідність змінного струму для структури PVA/PVP збільшуються із збільшенням вмісту наночастинок MnO_2. Діелектрична проникність і діелектричні втрати зменшуються, тоді як електропровідність змінного струму зростає зі збільшенням частоти. Оптичні характеристики наноструктур PVA/PVP/MnO_2 показали збільшення поглинання зі збільшенням вмісту наночастинок MnO_2. Ширина непрямої енергетичної забороненої зони PVA/PVP зменшується зі збільшенням вмісту наночастинокMnO_2. Оптичні константи змінюються зі збільшенням вмісту MnO_2. Результати застосування датчика тиску на основі наноструктур PVA/PVP/MnO_2 показали, що електрична ємність (Ср) збільшується зі збільшенням прикладеного тиску.

Ключові слова: MnO_2, сенсор тиску, заборонена зона, діелектрична стала, провідність.